International Journal of Hydrogen Energy 46 (2021), 22180-22194 (author version)

1D energy, exergy, and performance assessment of turbocharged diesel/hydrogen RCCI engine at different levels of diesel, hydrogen, compressor pressure ratio, and combustion duration

Hadi Taghavifar[1*], *Arash Nemati*[2], *Francisco J. Salvador*[3], *Joaquin De la Morena*[3]

1) Department of Mechanical Engineering, Faculty of Engineering, Malayer University, Malayer, Iran
2) Department of Mechanical Engineering, Technical University of Denmark, Nils Koppels Alle, 2800 Kgs, Lyngby, Denmark
3) CMT-Motores Térmicos, Universitat Politècnica de València, Spain

Abstract

There is a growing concern on the feasibility of new generation of internal combustion engines in a low-temperature and efficient way that can meet the emission regulations while maintaining the desirable power performance. This requires the controllability and flexibility over the ignition and reactivity within the cylinder by handling two fuels with different chemical reaction intensity. In this research, the reactivity controlled compression ignition (RCCI) turbocharger-assisted engine is proposed that operates with diesel-hydrogen fuels. After calibration and model validation, the effect of compression ratio of turbocharger, hydrogen energy share, diesel mass per cycle, and combustion duration on temperature rise, entropy, pressure, heat release, and engine performance is evaluated. The design variables effects on the exergy share of work, heat, exhaust loss, irreversibility, and exergy performance coefficient (EPC) are assessed and analyzed. Increasing the compressor pressure ratio can significantly increase the engine power and reduce the fuel consumption. It is proved that turbocharging can reduce the entropy generation and thereby reduce the irreversibility. The lower diesel injection is favored in terms of the work exergy and the EPC.

Keywords: *1D thermodynamic simulation; Diesel; Exergy; Hydrogen; RCCI; Turbocharging*

1. Introduction

The research on automotive engineering has been recently centered around the powertrain reconfiguration to modify and manipulate the combustion mode and chemical kinetics of the in-cylinder processes from one hand [1, 2]. On the other side, finding a surrogate fuel injection with gaseous hydrogen and compressed natural gas (CNG) or methane has gained momentum in internal combustion engines in an attempt to bring the emissions under Euro 5/6 limit legislation [3-5]. This is because hydrogen and methane have zero or ultra-low carbon in their composition, resulted in low soot and unburned hydrocarbon (UHC), as well as CO_2 reduction.

Within the compression ignition (CI) framework, the homogenized charge compression ignition (HCCI) and reactivity controlled compression ignition (RCCI) combustion modes have been developed to have better control on ignition and injection processes. In RCCI configuration, different operational parameters are involved such as fuel ratio between low and high reactivity sensitivity [6], injection strategy and timing [7], exhaust gas recirculation (EGR) ratio [8], compression ratio [9], etc. Moreover, the binary fuel selection for the port fuel and direct in-cylinder fuel injection of RCCI engine has been undertaken in the literature, where the most applied combinations are gasoline/diesel [10], CNG/diesel [11], methanol/diesel [12].

Meanwhile, 1D thermodynamic modeling of powertrain arrangement has been gaining attention due to fast analyze of different engine configurations with various fuels without resorting complexities of chemical kinetics. In this context, Ayad et al. [13] performed a numerical study on spark ignition (SI) ethanol fueled engine with hydrogen enrichment to survey the effect of hydrogen energy share on emission and engine performance metrics. It was summarized that with increase of hydrogen share, in general, the thermal efficiency raised while emissions declined. The energy and exergy analysis of a diesel engine is reported in [14] where the effects of the combustion characteristic quantities on energy efficiency are explored. They argued that as the combustion quality increases the irreversible exergy loss also increases which is concomitant with increasing the heat loss from the exhaust. An improved heat transfer model with boiling effect consideration is developed in the work of Zhang et al. [15] on the performance of diesel engine with different fuels of diesel and rapeseed methyl ester. Based on the obtained observations, increasing the inlet pressure causes a fuel consumption decrease.

Exergy analysis is considered as a key tool to evaluate the performance of the combustion engines since it is an index of the quality of energy or availability of energy that can be converted to useful work. Therefore, in the recent years, many studies are conducted on the exergy analysis of the combustion engines. Rangasamy et al. [16] carried out energy and exergy analysis for oxygenated bio-fuels based dual fuel reactivity controlled compression ignition (DFRCCI) engine. They concluded that incomplete combustion loss decrease by using biodiesel instead of diesel due to increased fuel stratification caused by the physical properties of biodiesel and in-cylinder temperature. Mahabadipour et al. [17] applied an exergy methodology to study a dual fuel engine by a multi-zone simulation. Based on their results, about 99% of the total exergy input into the engine is chemical exergy of the fuels (methane and diesel) and only 1% is supplied by physical exergy. Furthermore, in their studied engine, about 41-42% of the total input exergy is destroyed by irreversibilities. They also mentioned that the exergetic efficiency should be considered to find the most effective operating conditions. Eyal and Tartakovsky conducted an exergy analysis of a reforming-controlled compression ignition engine [18]. Their results clarified that the exergy efficiency optimization reaches up to 7.1 percent and by increasing the compression ratio from 16:1 to 18:1, exergy efficiency could be optimized about 9.2 percent. They also found that about 33% of the total input exergy is destroyed due to combustion processes inside the cylinder, and approximately 5% is destroyed in the reforming system. An energy and exergy analysis is carried out for a turbocharged hydrogen internal combustion engine by Wang et al. [19]. The results clarified that the exergy efficiency of the coolant energy does not exceed 5%, and the exergy efficiency of the exhaust energy can reach up to 23%. Li et al. [20] conducted a comprehensive investigation on the exergy destruction sources in different combustion regimes i.e. including conventional diesel combustion (CDC), homogeneous charge compression ignition (HCCI), and reactivity controlled compression ignition (RCCI). The results revealed that the exergy destruction due to heat and mass for CDC is bigger than HCCI and RCCI due to the more homogeneous distribution of fuel/air in the low temperature combustion regimes such as HCCI and RCCI. Also, they concluded that the exergy destruction due to port fuel injection is smaller than that due to fuel direct injection into the cylinder. Feng et al. [21] conducted an exergy analysis on the effects of intake conditions for a low temperature combustion with a toluene reference fuel. It is found out, as the intake temperature rises, irreversibility decreases. Furthermore, the percentage of irreversibility and working exergy increase obviously with compression ratio increasing, which is opposite with the enhanced speed condition. The effect of engine operating conditions and fuel on the energetic and exergetic efficiency of a heavy duty engine is investigated by Wang et. Al [22]. They concluded that the water injection leads to a significant reduction in the first and second law efficiencies and increases the exergy destruction. The first law exhaust loss increased when adding water to the combustion process due to the increase in the exhaust enthalpy and flow mass, however, the second law exhaust loss decreased due to the drop in the exhaust temperature. Therefore, there was no benefit for a WHR system with water injection.

The RCCI engine configuration with hydrogen/diesel combination is practiced in this research project by adopting 1D thermodynamic modeling. The energy balance and entropy generation for different operational parameters of the engine and then the second thermodynamic law is applied to realize how these parameters affect the exergy, irreversibility, and exergy performance coefficient (EPC) terms. The study of simplified thermodynamic cycle simulation of turbocharged RCCI engine with compressor pressure ratio, hydrogen and diesel mass variation on engine performance and exergy analysis lacks enough attention in the literature and this is an effort to cover this important research area. For a better outline of the step-by-step procedure of the current study, the workflow diagram is illustrated in Fig. 1.

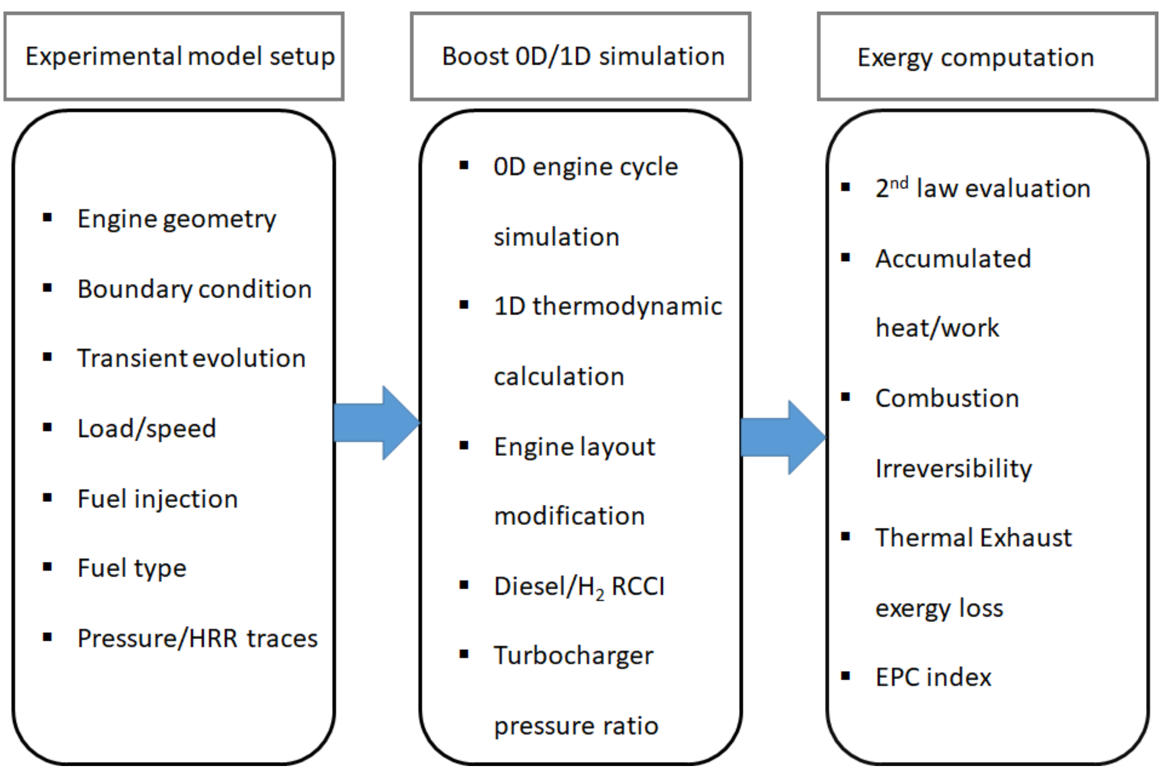

Figure 1. Detailed schematic of the workflow

2. Methodology

A series of thermodynamic and mathematical modeling are incorporated in the AVL-Boost platform to account the detailed realistic processes occurring in the component and mechanical interconnection between the elements. The pipe flow is assumed one dimensional and the required data transfer is according to the gas dynamic equations. In the post-processing phase, the output data i.e. pressure, temperature, mass flow, species concentration, and etc. are served for exergy evaluations.

2.1 Engine model description and configuration

As mentioned before, AVL-Boost software is employed to model the combustion process in the engine. A 1.8 L, 4-stroke Ford diesel engine is used as a baseline model in this study and then is modified and reconfigured by the incorporation of a H_2 injector before plenum and cylinders. The basic high speed direct injection (HSDI) diesel engine specifications and operating conditions are presented in Table 1. In this study, all of the gases are considered as ideal gas and therefore, the gas properties depend on temperature and gas composition. The gas leakage loss from the cylinder rings is ignored.

Table 1. Engine specifications

Engine specs	Value/comment
Manufactured	1.8L Ford
Displacement	438 (cm^3/cylinder)

Rated speed	1500 (rpm)
Number of cylinders	4
Bore × Stroke	82.5 × 82 (mm)
Compression ratio	19.5:1
Conrod	130 (mm)
Clearance	0.86 (mm)
Nozzle geometry	5×0.15 (mm)

A schematic of engine simulation is presented in Fig. 2. The powertrain layout and mechanical connections are displayed where a turbocharger provides compressed air flow and an H_2 injector injects hydrogen gas into the compressed air. The hydrogen and air are well mixed before the cylinder intake, then diesel is directly injected into the cylinder volume.

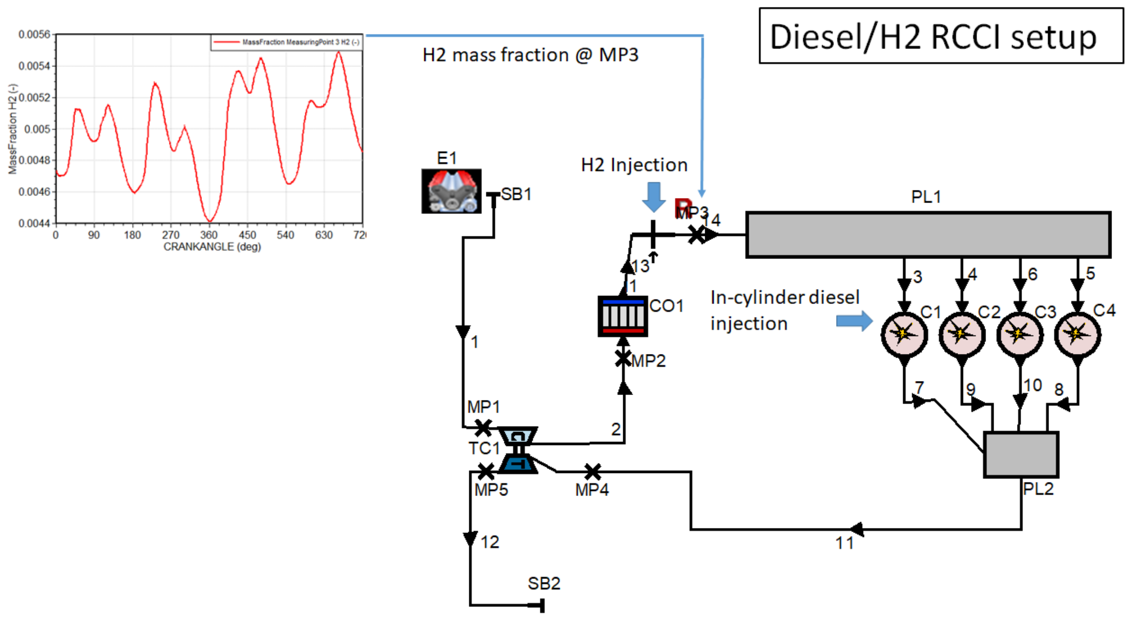

Figure 2. The proposed RCCI engine layout (modified HSDI diesel engine)

The cylinder volume is defined as the control volume in the mathematical modeling. The conservation of energy, mass and the ideal gas law are employed in the modeling. The energy balance as a function of the angle of the crankshaft can be written as follow:

$$\frac{d(m_c u)}{d\theta} = \frac{dQ_f}{d\theta} - \sum \frac{dQ_W}{d\theta} - p_c \frac{dV}{d\theta} + \sum h_e \frac{dm_e}{d\theta} - \sum h_s \frac{dm_s}{d\theta} - \sum h_{BB} \frac{dm_{BB}}{d\theta} - q_{ev} f \frac{dm_{ev}}{d\theta} \quad (1)$$

where, m_c is the mass inside the cylinder, u is the specific internal energy, p_c is the cylinder pressure, Θ is the crank angle, V is the cylinder volume, Q_F is the heat released by the fuel, Q_W is the heat loss to the walls, q_{ev} is the fuel specific heat of vaporization, m_{BB} is the blow-by mass and h_{BB} is enthalpy of the blow-by gases.

Mass is also conserved inside the cylinder. The mass balance can be presented as follow:

$$\frac{dm_{total}}{d\theta} = \sum \frac{dm_i}{d\theta} - \sum \frac{dm_e}{d\theta} - \frac{dm_{BB}}{d\theta} + \frac{dm_{ev}}{d\theta} \tag{2}$$

where, m_{total} is the total cylinder mass, m_i is the input mass, m_e is the exhaust mass and m_{ev} is the evaporated mass.

Due to considering ideal gas assumption for the in-cylinder gases, the ideal gas equation relates the pressure with volume, mass and temperature:

$$p_c = \frac{1}{V} m_c R_0 T_c \tag{3}$$

Then, the equation for temperature can be solved by Rang-Kutta method and by the calculated temperature, the pressure inside the cylinder can be calculated.

The two-zone Wiebe combustion model is used which calculates the burned fuel mass fraction as a function of crank angle [23, 24]. The heat transfer loss is one the most important losses in the combustion engines which needs a proper attention. In this study the following equation is used to calculate the heat transfer as a function of crank angle [25]:

$$\frac{\delta Q_{conv}}{d\theta} = \frac{1}{6N} h_w A_i (T_c - T_{wi}) \tag{4}$$

where, A_i is the combustion chamber surface area, N is the engine rotational speed, h_w is the heat transfer coefficient, T_c is the bulk gas temperature inside the cylinder and T_{wi} is the cylinder wall temperature. AVL-Boost uses the Woschni's equation to calculate the heat transfer coefficient.

2.2 Exergy model

The key concept of second-law analysis is 'availability' (or exergy). The availability content of material represents its potential to do useful work. Unlike energy, exergy can be destroyed which is the result of such phenomena as combustion, friction, mixing, and throttling. The exergy balance in the cylinder can be formulated as follows [26]:

$$\frac{dA_{cyl}}{d\phi} = \frac{\dot{m}_i b_i^{tm} - \dot{m}_o b_o^{tm}}{N} - \frac{dA_l}{d\phi} - \frac{dA_w}{d\phi} + \frac{dA_f}{d\phi} - \frac{dI}{d\phi} \tag{5}$$

In the above equation, $\dot{m}_i$ and $\dot{m}_o$ are the incoming and outgoing flow rates, respectively, b_i^{tm} and b_o^{tm} refer to their thermo-mechanical exergy which is defined as follow [26, 27]:

$$b^{tm} = (h - h_0) - T_0(s - s_0) \tag{6}$$

In Equation (5), $\frac{dA_l}{d\phi}$ represents the exergy of heat transfer to the cylinder walls on the basis of crank angle degree. It can be calculated as follow [26, 28]:

$$\frac{dA_l}{d\phi} = \frac{dQ_l}{d\phi}\left(1 - \frac{T_0}{T_{cyl}}\right) \tag{7}$$

where, $\frac{dQ_l}{d\phi}$ is the heat transfer rate to the cylinder walls on the basis of crank angle degree and T_{cyl} is the instantaneous temperature of the cylinder gasses, which are available from the engine simulation and energy analysis. In the exergy balance equation, the term of $\frac{dA_w}{d\phi}$ represents the indicated work transfer. In fact, it can be defined as the value of output exergy from the cylinder associated with the indicated work [26]:

$$\frac{dA_w}{d\phi} = \left(P_{cyl} - P_0\right)\frac{dV}{d\phi} \tag{8}$$

where $\frac{dV}{d\phi}$ states the rate of cylinder volume change based on crank angle degree and P_{cyl} is the instantaneous cylinder pressure which both are calculable by the first law analysis in the engine processes. The burned fuel exergy on the crank angle basis can be calculated as following [26]:

$$\frac{dA_f}{d\phi} = \frac{dm_{fb}}{d\phi} a_{fch} \tag{9}$$

where a_{fch} represents the chemical fuel exergy and for a blend composed of three different fuels this equation can be written as follow:

$$\frac{dA_f}{d\phi} = \frac{dm_{fb1}}{d\phi} a_{fch1} + \frac{dm_{fb2}}{d\phi} a_{fch2} + \frac{dm_{fb3}}{d\phi} a_{fch3} \tag{10}$$

The chemical exergy of substances in the environment (e.g. fuel, sulfur, combustion products such as NO or OH, etc.) can be evaluated by considering an idealized reaction of the substance with others with the known chemical exergies [29]. This chemical exergy of the fuel can be expressed on a molar basis as follow [26, 29]:

$$\overline{a}_{fch} = \overline{g}_f (T_0, P_0) - \left(\sum_p x_p \overline{\mu}_p^0 - \sum_r x_r \overline{\mu}_r^0 \right) \tag{11}$$

where index *p* denotes products (CO_2, H_2O, CO, etc.) and index *r* is the reactants (fuel and O_2) of the (stoichiometric) combustion process, T_0 and P_0 are the dead state temperature and pressure, and the over bar denotes properties on a mole basis. For liquid fuels of the general type $C_zH_yO_pS_q$, applicable in internal combustion engines, the chemical exergy of fuel can be expressed as follows (on a kg basis) [30]:

$$a_{fch} = LHV\left(1.0401 + 0.01728\frac{y}{z} + 0.0432\frac{p}{z} + 0.2196\frac{q}{z}\left(1 - 2.0628\frac{y}{z}\right)\right) \tag{12}$$

where *LHV* is the fuel lower heating value.

The $\frac{dI}{d\phi}$ term in exergy balance equation represents the rate of irreversibility production in the cylinder, which includes combustion, viscous loss, turbulence, mixing, etc. According to Dunbar and Lior [31], a combustion reaction has four major sources of internal irreversibility. They are:

- A chemical diffusion process in which air and fuel molecules are drawn together.
- Combustion of the fuel-air mixture (thermo-chemical reaction).
- Internal energy exchange through molecular collisions amongst the products and radiation heat transfer amongst product constituents due to unequal heat distribution.
- Mixing process whereby reactants mix before combustion, and products mix with reactants during combustion due to proximity.

Since the contribution of combustion in irreversibility production is more than 90% [32, 33], in the present study, only the combustion irreversibility is taken to evaluate the in-cylinder irreversibilities. The combustion irreversibilities on the crank angle basis can be given as [34, 35]:

$$\frac{dI}{d\phi} = -\frac{T_0}{T_{cyl}}\sum_j \mu_j \frac{dm_j}{d\phi} \tag{13}$$

where subscript *j* includes all reactants and products. For ideal gases, $\mu_j = g_j$ and for fuels $\mu_f = a_{fch}$ .Aforementioned equations can be solved by the numerical methods in order to evaluate the second-law terms in an engine cycle.

2.3 Validation and case setup

The validation of numerical modeling is performed according to baseline HSDI engine fueled with diesel at 1500 and 2500 rpm engine speeds. The in-cylinder mean pressure and heat release rate curves are taken for testing the robustness of the engine modeling in the output results prediction veracity. As shown in Fig. 3, the assembled engine with the input data and the adopted models is reliable with less than 4% deviation of the simulated data with the experimentally measured results [36, 37].

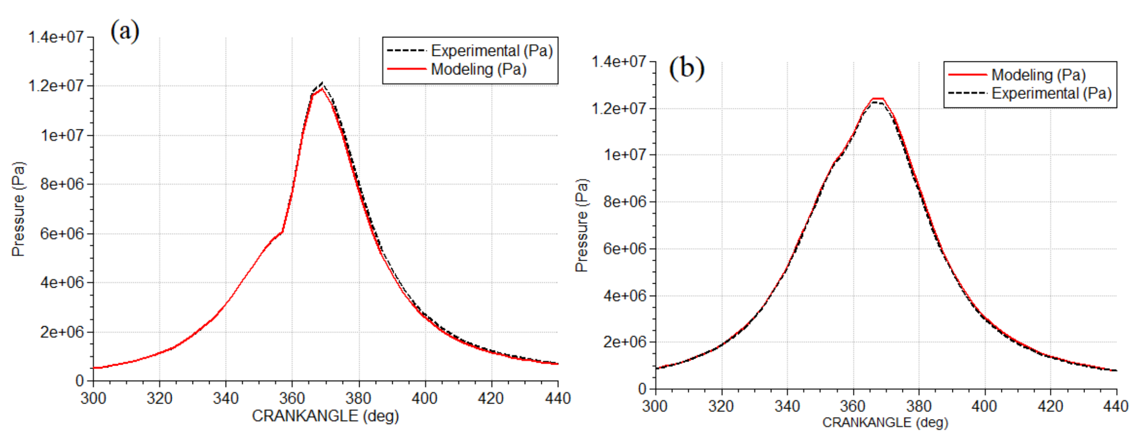

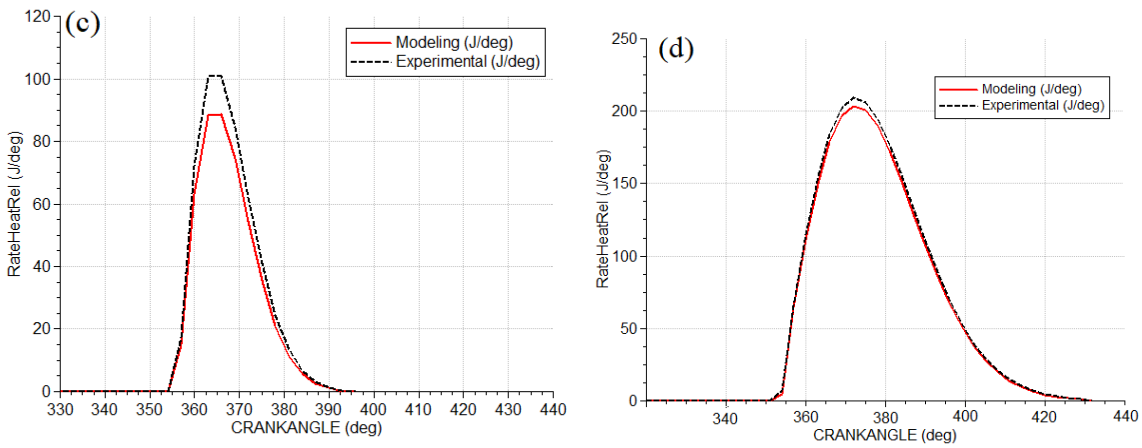

Figure 3. comparison of simulated vs. experimental data: (a) pressure @1500 rpm, (b) pressure @2500 rpm, (c) HRR @ 1500 rpm, (d) HRR @ 2500 rpm

The physical and chemical characteristics of the utilized fuels (diesel and hydrogen) as input data in the format of general species setup are gathered in Table 2. Meanwhile, Table 3 lists the under investigation operational parameters and the respective value levels for each case. In total, considering the four engine parameters along with three levels of variation, 9 cases are analyzed in the next chapter.

Table 2. Used fuel properties

Item	Diesel	Hydrogen
Molar mass (kg/kmol)	100.2	2.015
Lower heating value (MJ/kg)	42.83	120.043
Stoichiometric A/F ratio	15.16	34.273
Carbon/total mass ratio	0.839	0

Heat of evaporation (kJ/kg)	275.0	456.0
Density (kg/m^3)	837.0	0.089

Table 2. Parameter variation for the sensitivity analysis of operational condition in the RCCI mode

	CD (deg)	r_P (-)	m (mg)	Inj_m_cycle (mg/cycle)
Case1 (baseline)	36	1.2	31.3	10
Case2	56	1.2	31.3	10
Case3	76	1.2	31.3	10
Case4	36	2.0	31.3	10
Case5	36	2.8	31.3	10
Case6	36	1.2	11.3	10
Case7	36	1.2	21.3	10
Case8	36	1.2	31.3	20.0
Case9	36	1.2	31.3	30.0

3. Result and discussion

The direct injection of low-reactivity diesel fuel and port fuel injection of high-reactivity hydrogen fuel is investigated by manipulation of a conventional diesel engine. The amount of both fuels are varied to bring the reactivity of flow under control. The turbocharger compressor's pressure ratio and the combustion length are additional factors for flexibility of chemical kinetics and combustion management.

3.1. Combustion duration

The combustion duration is often determined on the engine type, combustion system, turbocharged/naturally aspirated air induction model, and other operating conditions. There are available engine speed-load maps to detect vibe combustion characteristic parameters. The combustion duration (CD) levels of 36 deg, 56 deg, and 76 deg are selected and its influence on pressure, heat release rate, entropy, and temperature rise is examined. In Fig. 4, as seen, the CD length can remarkably alter the pressure curve during early combustion period. The increase of combustion duration from 36 deg to 76 deg leads to a peak pressure drop from 12.5 MPa to 8.25 MPa. The same trend is noted for heat release rate (HRR) when CD has increased from 36 deg to 76 deg, the peak amount plummets from 86.34 J/deg to 34.16 J/deg. In both parameters, the combustion duration increment causes a slight higher pressure and heat release within late-combustion interval. Combustion duration increase results in lowering the intensity of combustion and more uniform distribution of energy during the expansion course.

Combustion is the main source of irreversibility and as can be appreciated in Fig. 4c, the longer CD of 76 deg makes higher entropy generation and energy quality degradation. After TDC, the entropy generation (increase) rises and then starts to decline. However, the more the combustion endures the more entropy is produced, which cause rapid exergy destruction. The rate of temperature rise is shown in Fig. 4d for different CD cases. The temperature fluctuation for CD=36 deg is more intense (124.26 K/deg) since in a short time there is little opportunity for chemical reaction and the huge temperature gradient is observed.

(a)

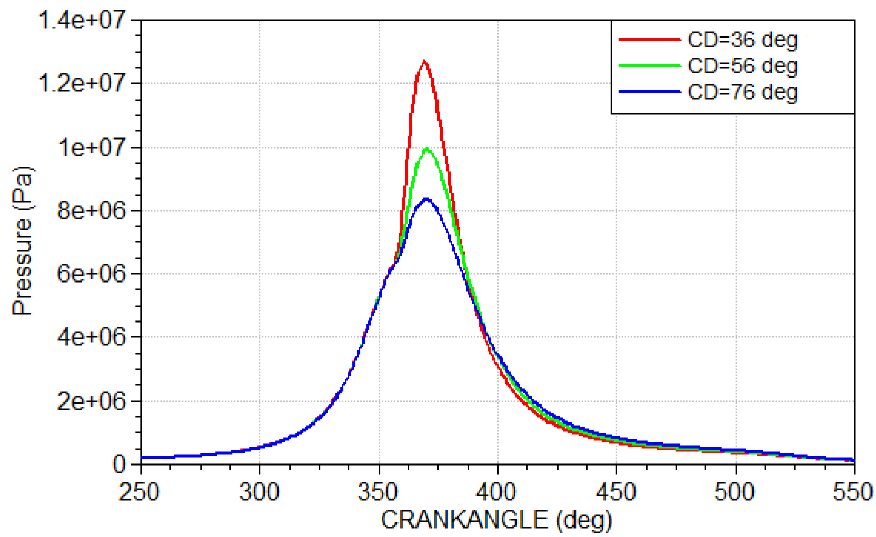
1.4e+07
1.2e+07
1e+07
8e+06
6e+06
4e+06
2e+06
0
Pressure (Pa)
250
300
350
400
450
500
550
CRANKANGLE (deg)
CD=36 deg
CD=56 deg
CD=76 deg

(b)

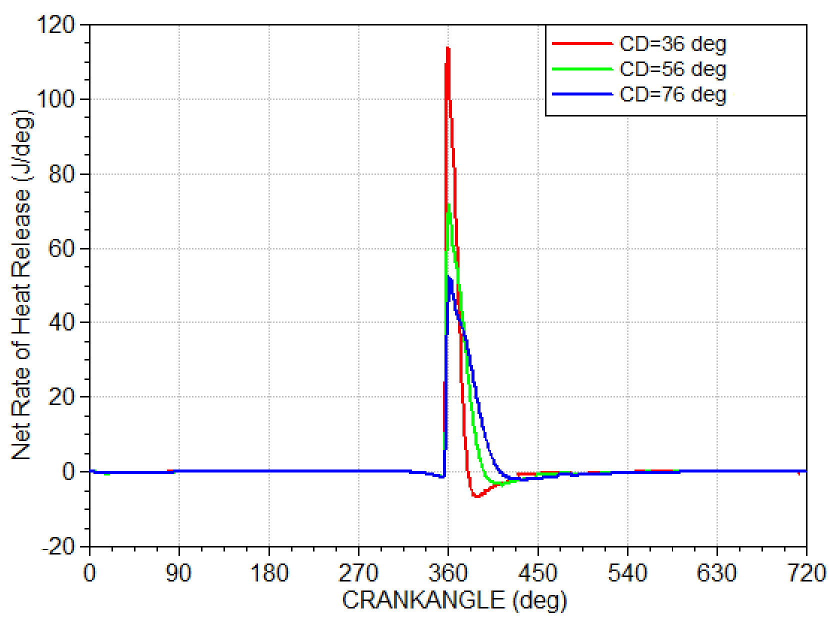
120
100
80
60
40
20
0
-20
Net Rate of Heat Release (J/deg)
0
90
180
270
360
450
540
630
720
CRANKANGLE (deg)
CD=36 deg
CD=56 deg
CD=76 deg

(c)

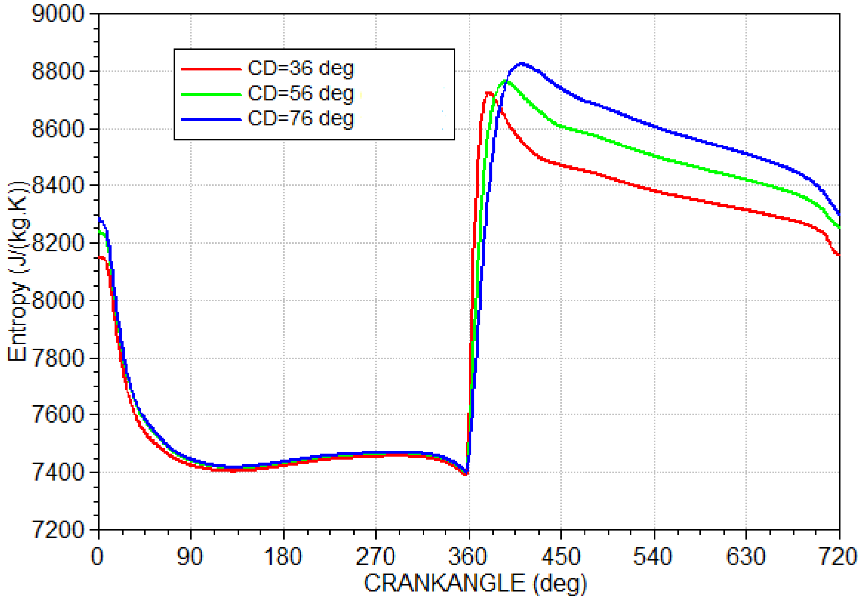

(d)

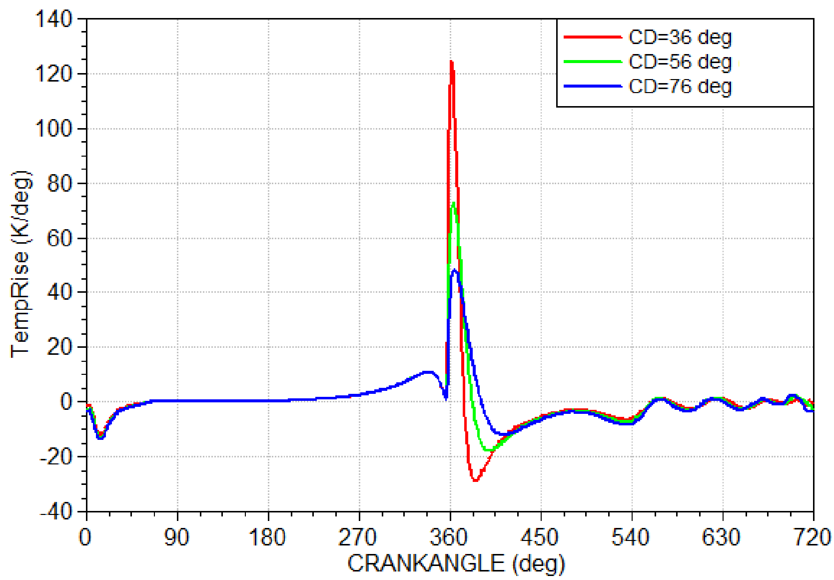

Figure 4. Effect of combustion duration on (a) pressure, (b) HRR, (c) entropy, (d) temperature rise rate curves during CA evolution

3.2. Turbocharger pressure ratio

Application of optimal compressor and turbine sizing for a turbocharged engine leads to a boosted performance of the system and the matching procedure is crucial for compressed air delivery to cylinder with the least energy loss. The compressor pressure ratio has been taken into account to assess the overall engine performance. This factor is estimated as:

$$r_P = \frac{P_m + \Delta P_{cooler}}{P_0 - \Delta P_{cleaner}} \tag{9}$$

where P_m is intake manifold pressure, ΔP_{cooler} inlet cooler pressure loss, P_0 the ambient pressure, and $\Delta P_{cleaner}$ the air cleaner pressure loss all in bar unit (cleaner component is not incorporated to the system here, thus $\Delta P_{cleaner}$=0).

Fig. 5 represents the variation of pressure, HRR, entropy, and temperature rise with different compressor pressure ratios at 1.2, 2.0, and 2.8 along CA. As expected, increasing the r_p affects the in-cylinder mean pressure and this change happens within all closed cycle from IVO to EVC, since the inducted air from inlet valve to thrusted out exhaust from outlet valve is compressed. This parameter affects the in-cylinder pressure significantly, that is to say 44.22% pressure peak is obtained for corresponding increase of 1.2 to 2.8 of r_p. The heat release rate of 1.2 r_p is marginally greater in early combustion and negligibly smaller than higher r_p. This is explained by the fact that higher r_p takes in more and denser air to cylinder and much more air absorbs of the reacted fuel.

Interestingly, the entropy generation for higher 2.8 compressor pressure ratio is lower that means efficient turbocharging prevents irreversibility thereby exergy can be promoted. Furthermore, the lower r_p results in higher peak of temperature rise due to lower mass of air, and for a fixed fuel amount, the temperature increases rapidly. In other words, the higher compressed air better resists against heat variation or energy flux, therefore damps the instabilities of the flow. This gradual change of temperature makes the process more gradual and entropy generation is reduced for r_p=2.8.

(a)

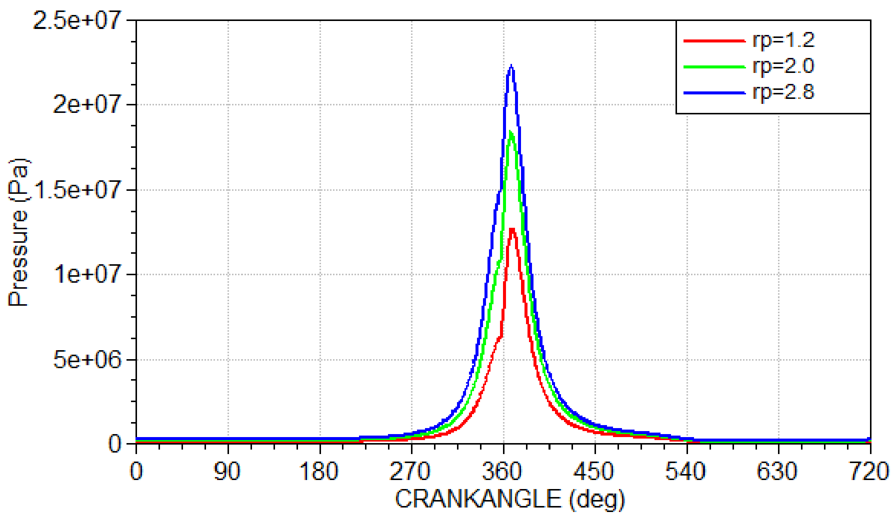

(b)

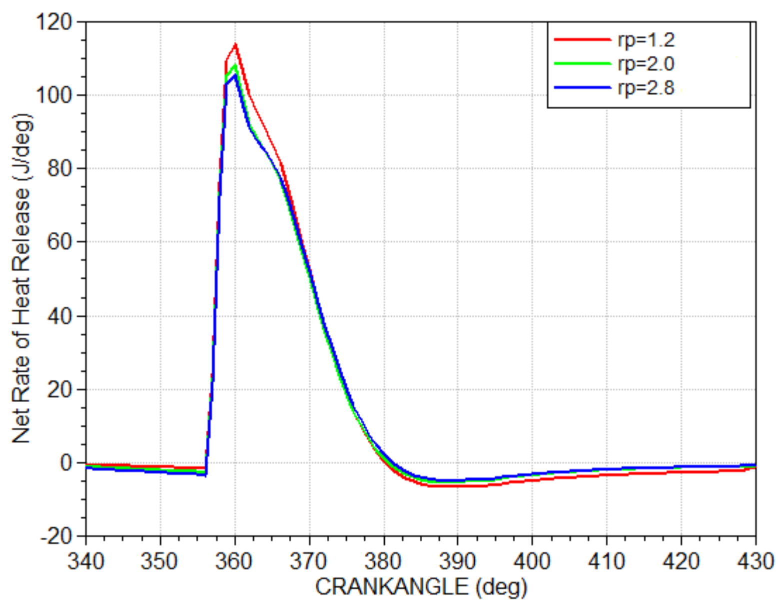

(c)

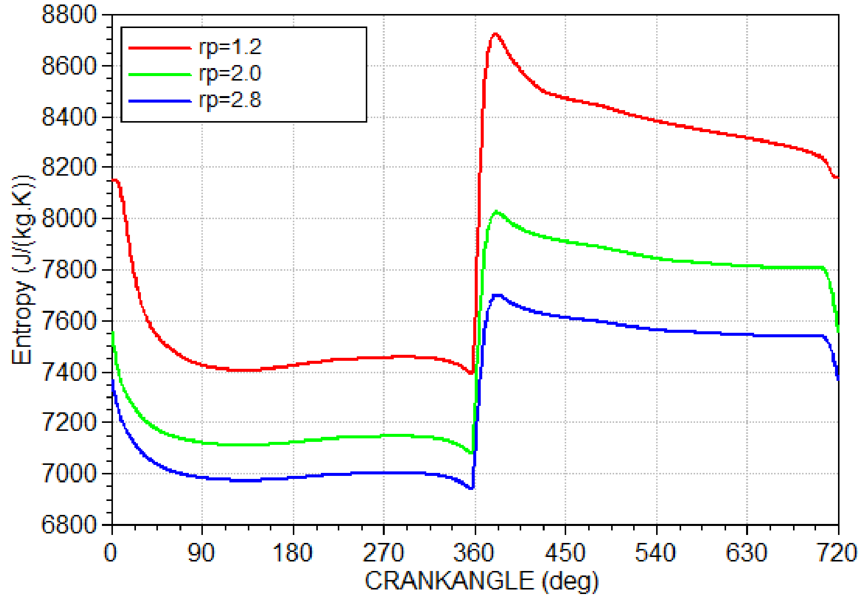

(d)

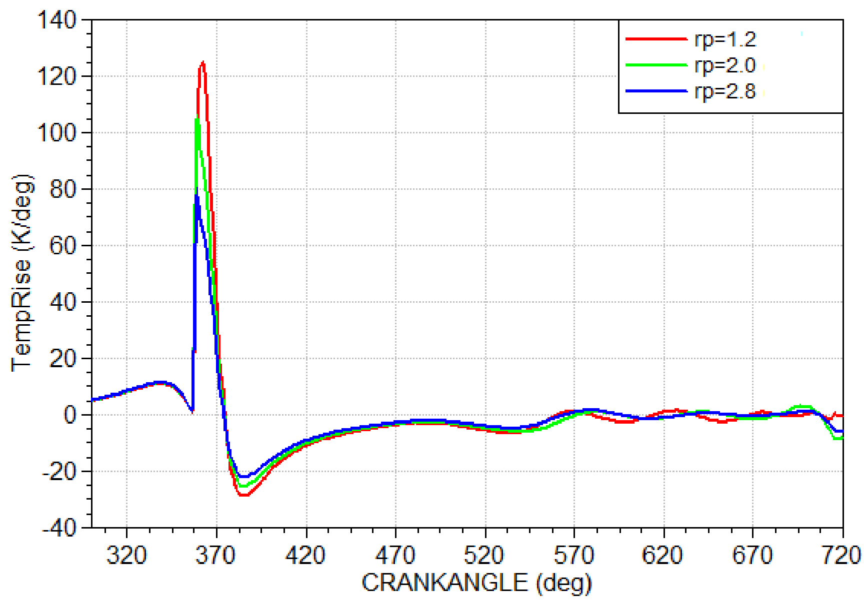

Figure 5. Effect of compressor pressure ratio on (a) pressure, (b) HRR, (c) entropy, (d) temperature rise rate curves during CA evolution

3.3. Diesel mass direct-injection to cylinder

Direct injection of diesel into cylinder is practiced with different diesel mass per cycle (11.3 mg/cycle, 21.3 mg/cycle, and 31.3 mg/cycle) while air/H_2 enriched charge are entered to the chamber through inlet valve. The pressure curves with respect to diesel mass are plotted in Fig. 6a and it is evident that the pressure curves demonstrate branching after injection of different diesel mass ratios. There is 21.5% peak pressure increase with 31.3 mg/cycle diesel injection compared to initial 11.3 mg/cycle diesel injection. The more fuel injected, the more chemical potential of fuel and more energy is released then the in-cylinder pressure rise sharply. The HRR graph in Fig. 6b reflects the higher energy of 31.3 mg/cycle diesel injection, which is roughly as double amount of energy released by 11.3 mg/cycle diesel injection.

The entropy variation during CA for different amounts of fuel injection is displayed and compared in Fig. 6c. The distinguishing feature is that the more fuel injection causes the more entropy generation and this means more fuel energy is wasted when higher diesel amount is injected. As seen, the entropy of 31.3 mg/cycle outstripped other cases from the fuel injection onward. According to Fig. 6d, the peak of temperature rise rate corresponds with 21.3 mg/cycle and the temperature variation for the highest diesel injection is marginally lower. It implies that more diesel injection does not guarantee fast temperature rise in the cylinder, however it induces the peak temperature.

(a)

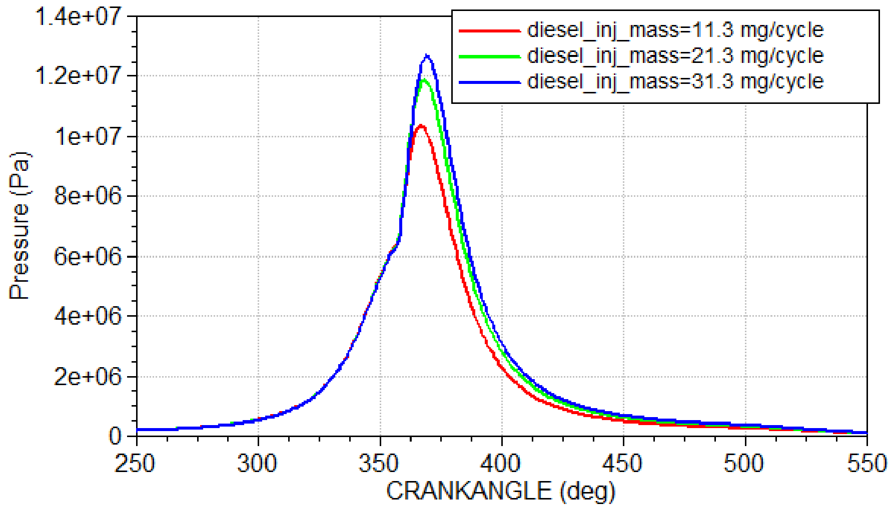
diesel_inj_mass=11.3 mg/cycle
diesel_inj_mass=21.3 mg/cycle
diesel_inj_mass=31.3 mg/cycle
Pressure (Pa)
CRANKANGLE (deg)

(b)

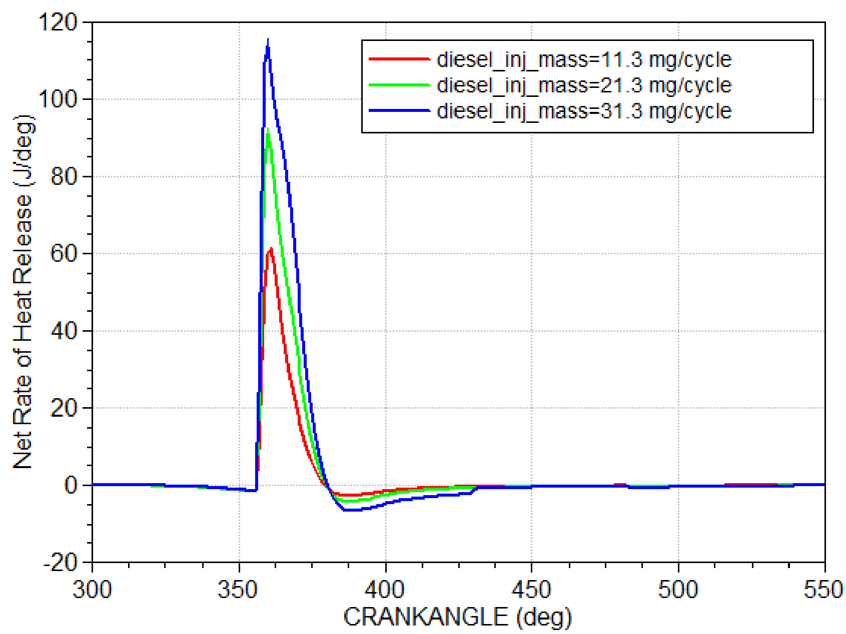
diesel_inj_mass=11.3 mg/cycle
diesel_inj_mass=21.3 mg/cycle
diesel_inj_mass=31.3 mg/cycle
Net Rate of Heat Release (J/deg)
CRANKANGLE (deg)

(c)

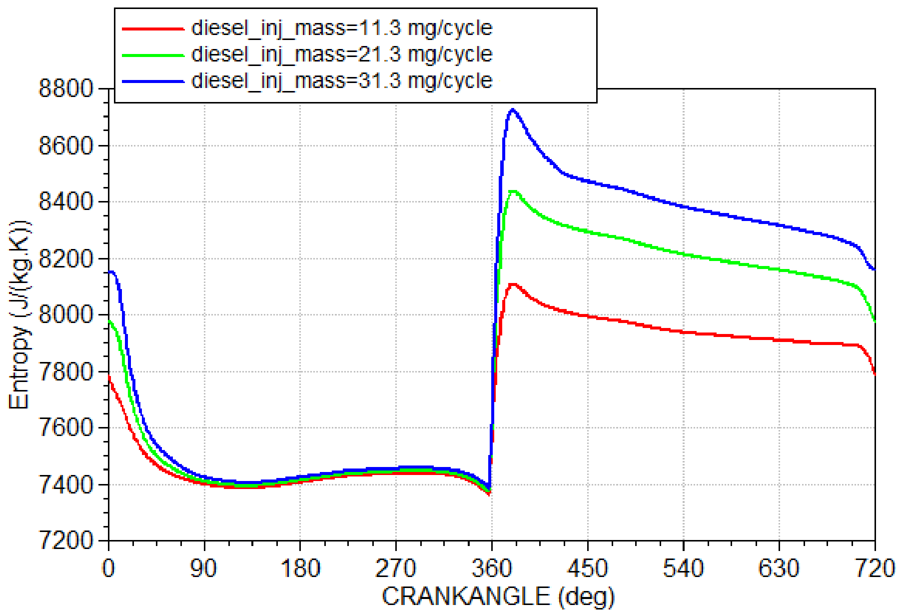

(d)

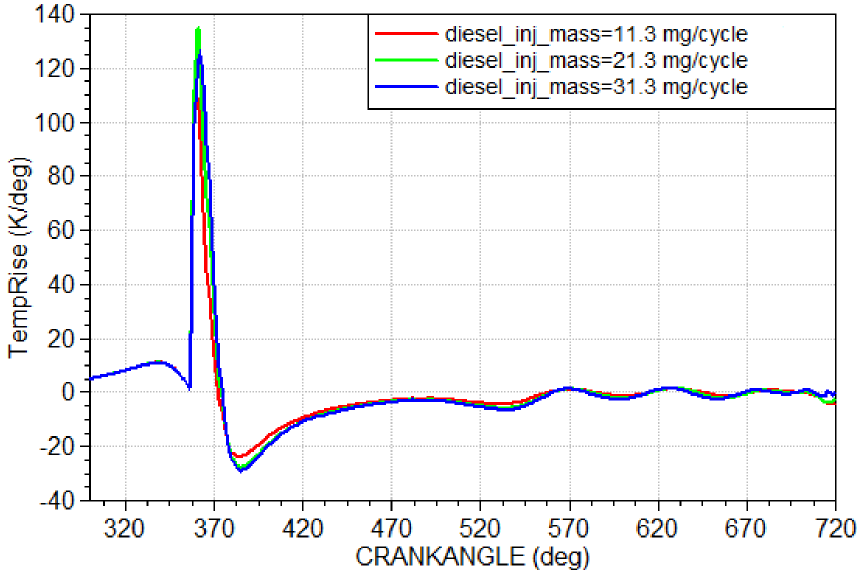

Figure 6. Effect of diesel mass DI on (a) pressure, (b) HRR, (c) entropy, (d) temperature rise rate curves during CA evolution

3.4. Hydrogen indirect injection (per H_2 energy share) to pipe

In this study, hydrogen energy share/fraction (HES) is selected to describe the hydrogen portion in mixture, which is defined and formulated as

$$HES(\%) = \frac{\dot{m}_{H_2}(LHV)_{H_2}}{\underbrace{\dot{m}_{H_2}(LHV)_{H_2} + \dot{m}_{diesel}(LHV)_{diesel}}_{E_{tot,chem}}} \times 100\% \tag{10}$$

This equation considers the ratio of hydrogen chemical energy to total energy of the mixed charge. The addition of hydrogen yields lower in-cylinder pressure as depicted in Fig. 7a. It is found that increasing HES contributes to low peak pressure. As also indicated in [38, 39] this is due to hydrogen ultra-low density (0.089 kg/m^3) and stoichiometric hydrogen-air energy content. On the other hand, though, according to Fig. 7b, the heat release of HES=12% is comparatively greater than lesser HES ratios. Given the substantially larger LHV for hydrogen than LHV of diesel, the peak HRR of 12% HES is 57.1% bigger than that of 4% HES case.

Regarding Fig. 7c, the variation of entropy for different HES ratios along CA. Unlike, diesel injection, in hydrogen addition, the entropy difference has been established throughout the CA since from the beginning (IVO) there was hydrogen+air. The higher HES ratio, the higher entropy values and therefore more energy fuel potential that cannot be exploited in the system for out power delivery. The change of HES, as seen in Fig. 7d, does not make any sensible TRR even in early combustion when the reaction occurs turbulently and temperature fluctuates in chaotic. The highest TRR is 124.8 K/deg of HES=4% that is closely followed by 116.28 K/deg of HES=8%. The low hydrogen share difference and low density of hydrogen in air is unable to cause a significant temperature gradient.

(a)

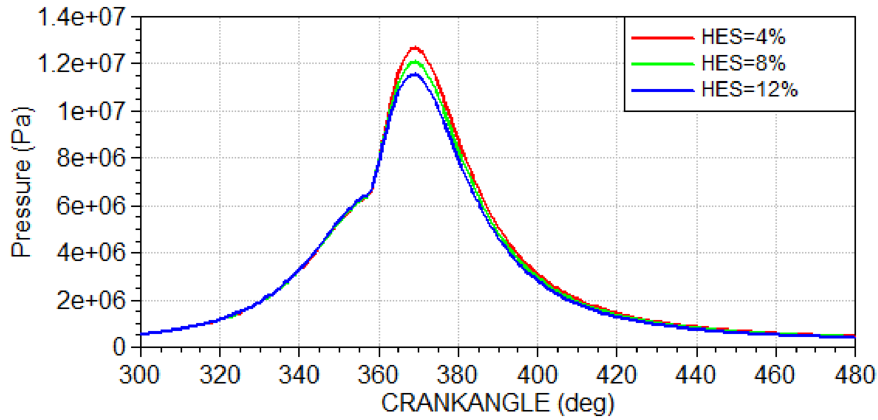
HES=4%
HES=8%
HES=12%
Pressure (Pa)
1.4e+07
1.2e+07
1e+07
8e+06
6e+06
4e+06
2e+06
0
300
320
340
360
380
400
420
440
460
480
CRANKANGLE (deg)

(b)

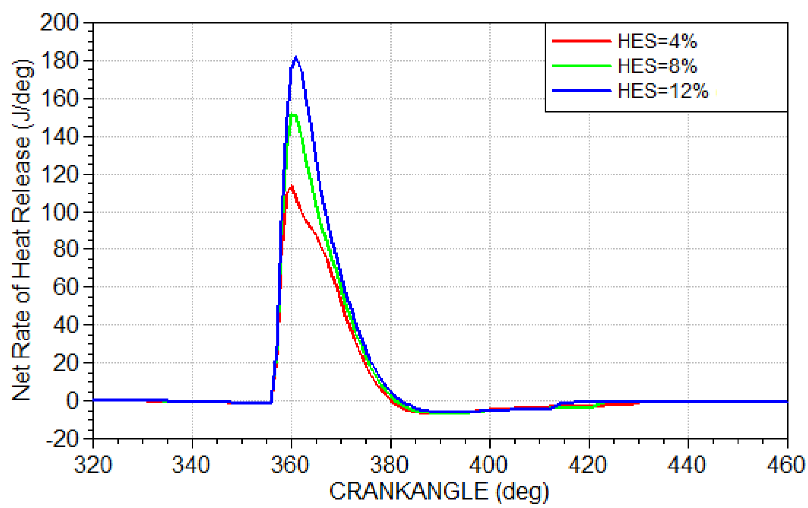
HES=4%
HES=8%
HES=12%
Net Rate of Heat Release (J/deg)
200
180
160
140
120
100
80
60
40
20
0
-20
320
340
360
380
400
420
440
460
CRANKANGLE (deg)

(c)

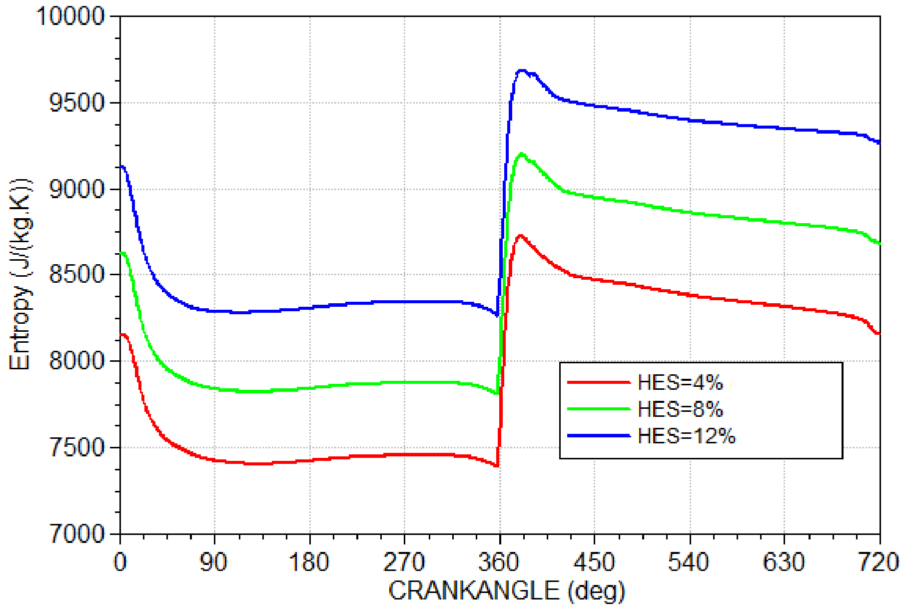

10000
9500
9000
8500
8000
7500
7000
Entropy (J/(kg.K))
0
90
180
270
360
450
540
630
720
CRANKANGLE (deg)
HES=4%
HES=8%
HES=12%

(d)

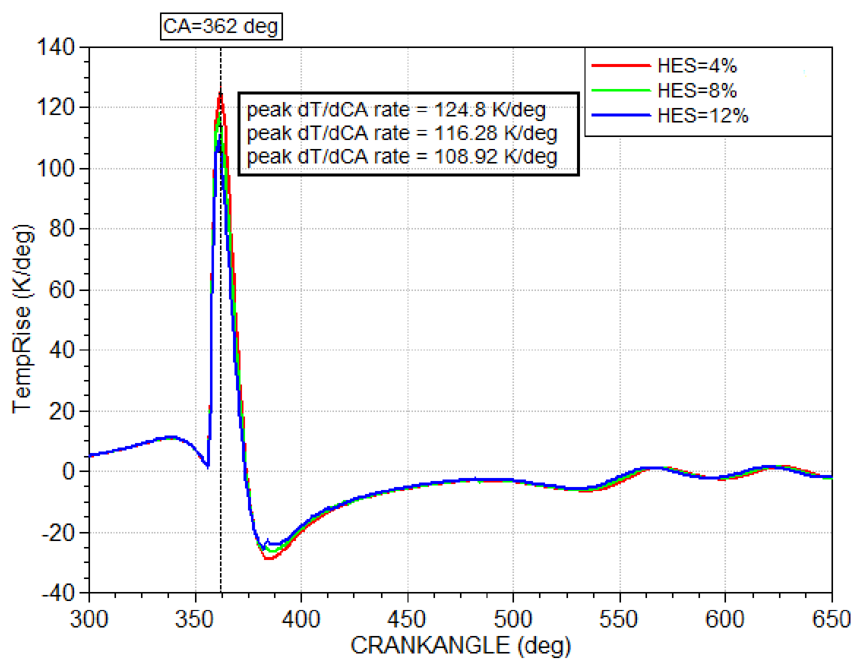

CA=362 deg
140
120
100
80
60
40
20
0
-20
-40
TempRise (K/deg)
peak dT/dCA rate = 124.8 K/deg
peak dT/dCA rate = 116.28 K/deg
peak dT/dCA rate = 108.92 K/deg
HES=4%
HES=8%
HES=12%
300
350
400
450
500
550
600
650
CRANKANGLE (deg)

Figure 7. Effect of HES on (a) pressure, (b) HRR, (c) entropy, (d) temperature rise rate curves during CA evolution

3.5. Engine power/thermal performance

Different cases collected in Table 3 are contrasted in different parameters of indicated power (IP), wallheat loss, indicated specific fuel consumption (ISFC), peak pressure rise (PPR), fuel energy, and exhaust gas loss. Case 1 as the reference case is marked and other cases are compared with case 1. According to Fig. 8a, increasing the CD, r_p and diesel DI lead to elevated power, while H_2 PFI decreases the indicated power of the system. Meanwhile, the most effective parameter in engine power boost is the compressor pressure ratio. The cylinder wall heat losses are an important criterion to assess the efficiency of the system. The wall heat losses decline when the r_p of the compressor increases since when the compressed air enters to cylinder, more of the released heat can be absorbed and lesser heat is transferred across the wall.

In Fig. 8b, increasing the combustion duration, r_p results in lower fuel consumption while diesel and H_2 amount increase obviously is conducive to more ISFC (note that cases 6 and 7 have lower diesel mass injection than baseline case 1). The increase of CD gives higher power due to the extended combustion and to keep the load constant ISFC must be decreased by 2.9% and 2.2% for case 2 and case 3. This also happens for compression pressure ratio when it rises the engine power then to keep a constant load, the fuel consumption declines (23.1% for case 4 and 25.6% for case 5). Increasing the H_2 fraction causes a considerable (the most) increase of ISFC since hydrogen has different physiochemical characteristics and extremely low density. Moreover, the compressed air induced by turbocharger can augment the PPR up to 31.2% since the compressed air can oxidize the fuel efficiently due to enriched oxygen content.

The graph of Fig. 8c provides data of fuel energy and as seen the hydrogen and diesel addition cause a growth in fuel energy, while change of operational factors makes a slight variation. The exhaust gas loss has a remarkable impact on exergy evaluation that defines how a system can be efficient to prevent energy loss and instead convert it to mechanical output. The CD elongation increases the exhaust gas loss since more exhausted gas would be produced and more time is provided for exhausting. The r_p increase of the turbocharger contributes to lowering the exhaust gas loss as much as 30.9% reduction. The lower diesel injection also leads to lower gas exhaust energy loss since the reactants molar/mass amount reduces and produces species will reduce. Further, H_2 increase corresponding to case 8 and case 9 shows an increase of exhaust gas since the hydrogen combustion increases the temperature and this high in-cylinder temperature generates free radicals and more reaction and species during the combustion.

(a)

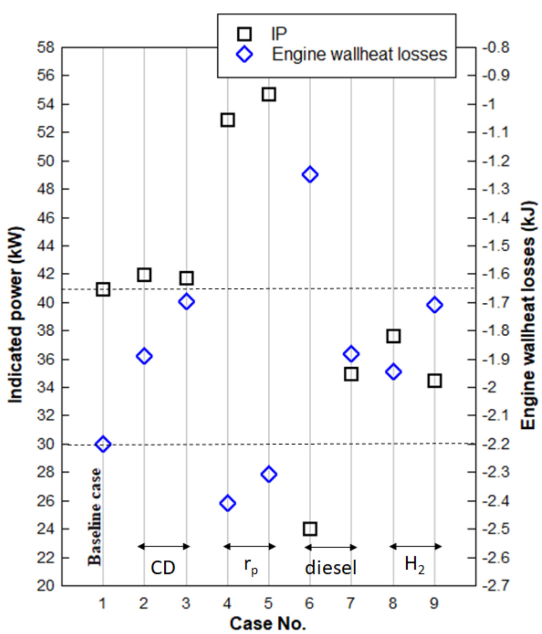

(b)

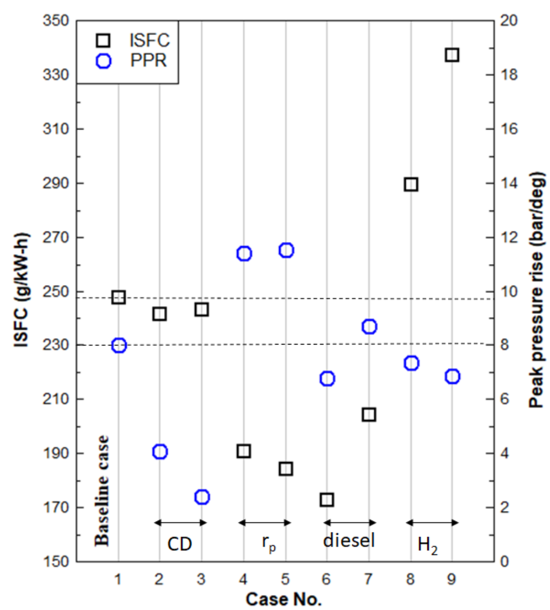

(c)

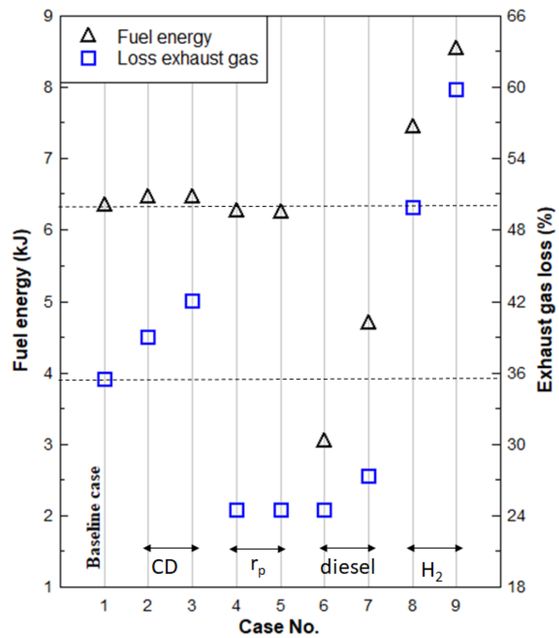

Figure 8. Variation of overall performance parameters for different cases: (a) IP and cylinder wall heat losses, (b) ISFC and PPR, (c) Fuel energy and exhaust gas loss

3.6. Exergy evaluation

Figure 9a gives a breakdown of exergy share for different under investigation cases. The highest portion of exergy is accumulated work, then in general view comes the accumulated heat exergy, the third rank goes to exhaust thermal exergy and finally the combustion irreversibility. Case 6 (diesel mass = 11.3 mg/cycle) demonstrates the highest work exergy fraction (47.8%) and the least combustion irreversibility of 3.62% that are desirable for the RCCI system exergetic performance. Since, hydrogen is involved in the charge, a more complete combustion is assured and excess diesel fuel combustion is wasted through exhaust and wall-heat transfer. Meanwhile, the 8% HES is optimal since the work exergy increases while the thermal exhaust decreases compared to base case 1. Another noteworthy point is that turbocharging has positive effect on increasing the work exergy although the combustion irreversibility increased. The combustion duration increase has substantially increased the exhaust thermal loss exergy since much of the exergy is wasted through the residual gas transport.

As to finalize the exergy assessment of different parametric cases of the RCCI configuration, the exergetic performance coefficient (EPC) is computed and plotted in Fig. 9b. The EPC of case 6 i.e. 11.2 (the least diesel DI) shows that in the RCCI dual-fuel hydrogen-diesel configuration gives the most work output per fuel energy and this gives the best cost-effective scheme in the proposed engine layout.

(a)

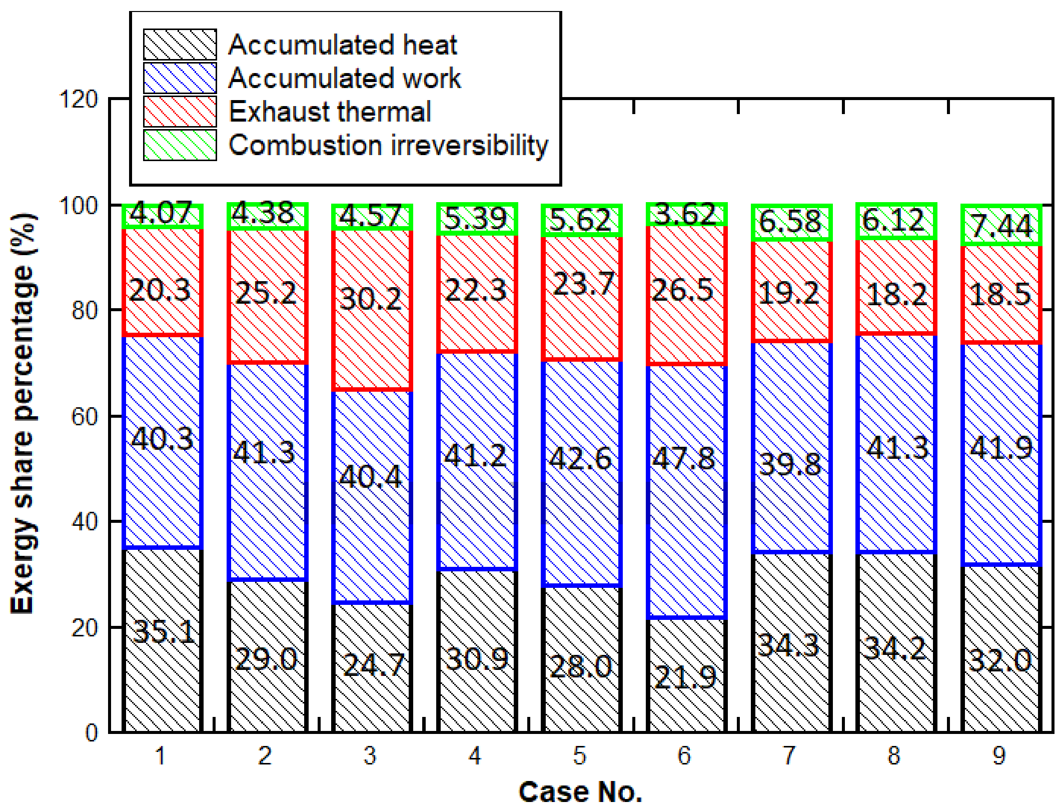

(b)

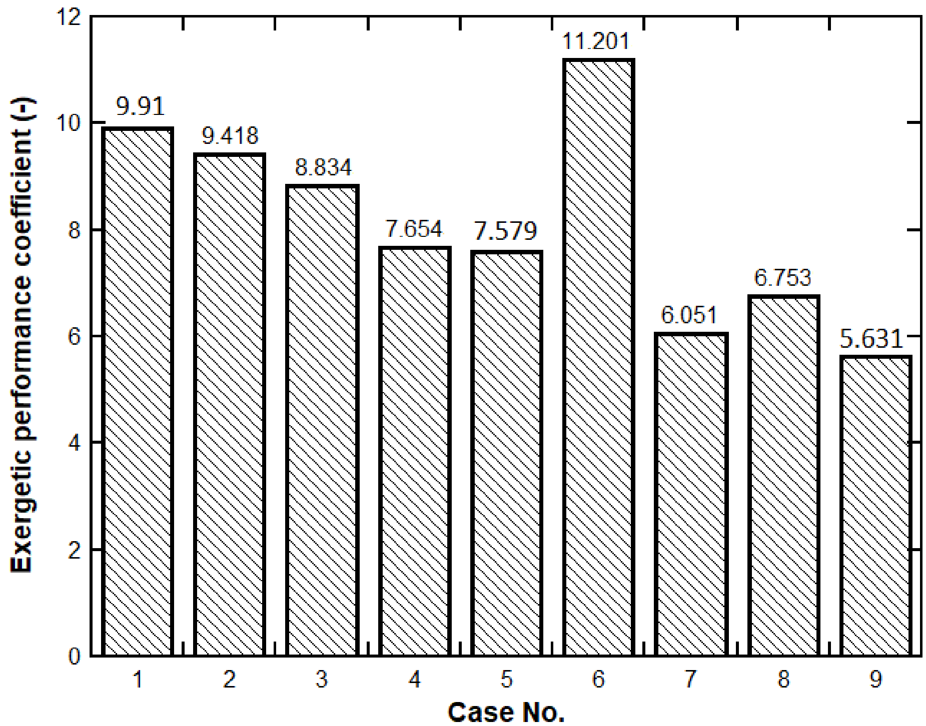

Figure 9. (a) Exergy share percentage of various exergetic terms, (b) EPC values for different parametric cases

4. Conclusion

In current investigation, the 1D thermodynamic modeling is performed within the AVL Boost platform to analyze various parameters change in energy and exergy frameworks. The reference engine is Ford 1.8 L CI engine and the modeling is implemented based on the base engine, then the engine is manipulated with incorporation of a turbocharger and H_2 port fuel injection before cylinder to account for the RCCI configuration. The combustion duration in cylinders, compressor pressure ratio, diesel mass injection, and hydrogen energy share are considered for the engine functioning assessment. The obtained data from previous phase served as input database for calculation of exergy and irreversibility terms. The summary of findings can be classified as below:

- The combustion duration increase results in reduced pressure, HRR, and TRR while the entropy increases. The increase of entropy is attributed to more heat loss due to endured combustion duration. However, a marginal rise in IP and ISFC decrease (about 2.9%) is observed. The exhaust gas loss increases with combustion duration, consequently the exhaust thermal exergy has been increased by 5.1% and 9.2% compared to baseline case since more heat is transported by the outflow from the system boundary. This factor also contributes to the combustion irreversibility increment.
- The increase of compressor pressure ratio in turbocharger is very effective in combustion chamber flow. It promotes the in-cylinder pressure and accumulated work exergy since the compressed air enhances the combustion quality. The indicated power is elevated to 53.1 kW and 55.9 kW from the initial 41.2 kW of baseline case that comes from a more efficient turbocharging. It has also deduced that higher r_p ratio narrows the entropy generation range denoting higher energy quality and prevention of exergy destruction.
- It is found that in RCCI mode, the lower diesel DI is preferable since the highest accumulated work exergy and EPC can be accomplished with the lowest diesel injection amount (case 6) since the entropy generation rapidly increases with high diesel mass injection. More diesel combustion caused strikingly higher HRR that this expedites the heat loss, exhaust gas exit, and combustion irreversibility.
- The highest hydrogen and diesel addition bring about the greatest combustion irreversibility shares with 7.44% and 6.58%. Interestingly, the hydrogen addition of HES=8% and HES=12% reduces the exhaust thermal exergy to 18.2% and 18.5%.

References

[1] Li, J., Yang, W. and Zhou, D., 2017. Review on the management of RCCI engines. *Renewable and Sustainable Energy Reviews*, *69*, pp.65-79.

[2] Lu, X., Han, D. and Huang, Z., 2011. Fuel design and management for the control of advanced compression-ignition combustion modes. *Progress in Energy and Combustion Science*, *37*(6), pp.741-783.

[3] Rahimi, H.M., Jazayeri, S.A. and Ebrahimi, M., 2020. Hydrogen energy share enhancement in a heavy duty diesel engine under RCCI combustion fueled with natural gas and diesel oil. *International Journal of Hydrogen Energy*.

[4] Moreno, F., Muñoz, M., Arroyo, J., Magén, O., Monné, C. and Suelves, I., 2012. Efficiency and emissions in a vehicle spark ignition engine fueled with hydrogen and methane blends. *International Journal of Hydrogen Energy*, *37*(15), pp.11495-11503.

[5] Bielaczyc, P., Woodburn, J. and Szczotka, A., 2014. An assessment of regulated emissions and CO2 emissions from a European light-duty CNG-fueled vehicle in the context of Euro 6 emissions regulations. *Applied Energy*, *117*, pp.134-141.

[6] Li, J., Yang, W.M., Goh, T.N., An, H. and Maghbouli, A., 2014. Study on RCCI (reactivity controlled compression ignition) engine by means of statistical experimental design. *Energy*, *78*, pp.777-787.

[7] Ma, S., Zheng, Z., Liu, H., Zhang, Q. and Yao, M., 2013. Experimental investigation of the effects of diesel injection strategy on gasoline/diesel dual-fuel combustion. *Applied Energy*, *109*, pp.202-212.

[8] Wu, Y. and Reitz, R.D., 2015. Effects of exhaust gas recirculation and boost pressure on reactivity controlled compression ignition engine at high load operating conditions. *Journal of Energy Resources Technology*, *137*(3).

[9] Hanson, R.M., Kokjohn, S.L., Splitter, D.A. and Reitz, R.D., 2010. An experimental investigation of fuel reactivity controlled PCCI combustion in a heavy-duty engine. *SAE international journal of engines*, *3*(1), pp.700-716.

[10] Kokjohn, S., Hanson, R., Splitter, D., Kaddatz, J. and Reitz, R., 2011. Fuel reactivity controlled compression ignition (RCCI) combustion in light-and heavy-duty engines. *SAE International Journal of Engines*, *4*(1), pp.360-374.

[11] Ebrahimi, M., Najafi, M., Jazayeri, S.A. and Mohammadzadeh, A.R., 2018. A detail simulation of reactivity controlled compression ignition combustion strategy in a heavy-duty diesel engine run on natural gas/diesel fuel. *International Journal of Engine Research*, *19*(7), pp.774-789.

[12] Zou, X., Wang, H., Zheng, Z., Reitz, R. and Yao, M., 2016. *Numerical study of the RCCI combustion processes fuelled with methanol, ethanol, n-butanol and diesel* (No. 2016-01-0777). SAE Technical Paper.

[13] Ayad, S.M., Belchior, C.R., da Silva, G.L., Lucena, R.S., Carreira, E.S. and de Miranda, P.E., 2020. Analysis of performance parameters of an ethanol fueled spark ignition engine operating with hydrogen enrichment. *International Journal of Hydrogen Energy*, *45*(8), pp.5588-5606.

[14] Yao, Z.M., Qian, Z.Q., Li, R. and Hu, E., 2019. Energy efficiency analysis of marine high-powered medium-speed diesel engine base on energy balance and exergy. *Energy*, *176*, pp.991-1006.

[15] Zhang, Z., Jiaqiang, E., Chen, J., Zhao, X., Zhang, B., Deng, Y., Peng, Q. and Yin, Z., 2020. Effects of boiling heat transfer on the performance enhancement of a medium speed diesel engine fueled with diesel and rapeseed methyl ester. *Applied Thermal Engineering*, *169*, p.114984.

[16] Rangasamy M, Duraisamy G, Govindan N. A comprehensive parametric, energy and exergy analysis for oxygenated biofuels based dual-fuel combustion in an automotive light duty diesel engine. Fuel. 2020 Oct 1;277:118167.

[17] Mahabadipour H, Srinivasan KK, Krishnan SR. An exergy analysis methodology for internal combustion engines using a multi-zone simulation of dual fuel low temperature combustion. Applied Energy. 2019 Dec 15;256:113952.

[18] Eyal A, Tartakovsky L. Second-law analysis of the reforming-controlled compression ignition. Applied Energy. 2020 Apr 1;263:114622.

[19] Wang X, Sun BG, Luo QH. Energy and exergy analysis of a turbocharged hydrogen internal combustion engine. international journal of hydrogen energy. 2019 Feb 26;44(11):5551-63.

[20] Li Y, Jia M, Kokjohn SL, Chang Y, Reitz RD. Comprehensive analysis of exergy destruction sources in different engine combustion regimes. Energy, 2018;149:697e708.

[21] Feng H, Wang X, Zhang J. Study on the effects of intake conditions on the exergy destruction of low temperature combustion engine for a toluene reference fuel. Energy Conversion and Management. 2019 May 15;188:241-9.

[22] Wang B, Pamminger M, Wallner T. Impact of fuel and engine operating conditions on efficiency of a heavy duty truck engine running compression ignition mode using energy and exergy analysis. Applied Energy. 2019 Nov 15;254:113645.

[23] Caton JA. An introduction to thermodynamic cycle simulations for internal combustion engines. NY,USA: John Wiley & Sons; 2016.

[24] A. Boost, Theory manual (AVL Boost v.2018.1), AVL List Gmbh, Graz-Austria.

[25] GUTIERREZ RHR. Diesel engine simulation and fault identification, Tese de doutorado. Thesis. Rio de Janeiro, Brazil: Universidade Federal do Rio de Janeiro; 2016.

[26] Haywood, R.W., Equilibrium thermodynamics for engineers and scientists, 1980.

[27] Taghavifar, H., Nemati, A., Salvador, F.J. and De la Morena, J., 2019. Improved mixture quality by advanced dual-nozzle, included-angle split injection in HSDI engine: Exergetic exploration. Energy, 167, pp.211-223.

[28] Nemati, A., Barzegar, R. and Khalilarya, S., 2015. The effects of injected fuel temperature on exergy balance under the various operating loads in a DI diesel engine. Int. J. Exergy, 17(1), pp.35-53.

[29] Bejan, A., 2016. Advanced engineering thermodynamics. John Wiley & Sons.

[30] Stepanov, V.S., 1995. Chemical energies and exergies of fuels. Energy, 20(3), pp.235-242.

[31] Dunbar, W.R. and Lior, N., 1994. Sources of combustion irreversibility. Combustion Science and Technology, 103(1-6), pp.41-61.

[32] Rakopoulos, C.D. and Giakoumis, E.G., 2006. Second-law analyses applied to internal combustion engines operation. Progress in energy and combustion science, 32(1), pp.2-47.

[33] Alkidas, A.C., 1988. The application of availability and energy balances to a diesel engine. Journal of Engineering for Gas Turbines and Power, 110(3), pp.462-469.

[34] Taghavifar H, Nemati A, Walther JH. Combustion and exergy analysis of multi-component diesel-DME-methanol blends in HCCI engine. Energy. 2019 Nov 15;187:115951.

[35] Rakopoulos C.D., Andritsakis E.C. DI and IDI Diesel Engines Combustion Irreversibility Analysis. 1993 American Society of Mechanical Engineers-Winter Annual Meeting, New Orleans, Louisiana, U.S.A., 1993. pp. 17-32.

[36] Taghavifar, H., Mardani, A., Mohebbi, A. and Taghavifar, H., 2014. Investigating the effect of combustion properties on the accumulated heat release of DI engines at rated EGR levels using the ANN approach. *Fuel*, *137*, pp.1-10.

[37] Taghavifar, H., Khalilarya, S. and Jafarmadar, S., 2015. Exergy analysis of combustion in VGT-modified diesel engine with detailed chemical kinetics mechanism. *Energy*, *93*, pp.740-748.

[38] Antunes, J.G., Mikalsen, R. and Roskilly, A.P., 2009. An experimental study of a direct injection compression ignition hydrogen engine. *International journal of hydrogen energy*, *34*(15), pp.6516-6522.

[39] JukneleviČius, R., Rimkus, A., Pukalskas, S. and Matijošius, J., 2019. Research of performance and emission indicators of the compression-ignition engine powered by hydrogen-Diesel mixtures. *International Journal of Hydrogen Energy*, *44*(20), pp.10129-10138.